Microchimica Acta (2020) 187: 236
https://doi.org/10.1007/s00604-020-4179-x

ORIGINAL PAPER

Development of a ZnCdS@ZnS quantum dots–based label-free electrochemiluminescence immunosensor for sensitive determination of aflatoxin B_1 in lotus seed

Chaonan Sun[1] · Xiaofang Liao[1] · Boyu Jia[1] · Linchun Shi[1] · Dingkun Zhang[2] · Ruilin Wang[3] · Lidong Zhou[1] · Weijun Kong[1]

Received: 14 December 2019 / Accepted: 24 February 2020 / Published online: 18 March 2020

Abstract

In this study, we designed a ZnCdS@ZnS quantum dots (QDs)–based label-free electrochemiluminescence (ECL) immunosensor for sensitive determination of aflatoxin B_1 (AFB_1). A Nafion solution assembled abundant QDs on the surface of a Au electrode as ECL signal probes, with specially coupled anti-AFB_1 antibodies as the capturing element. As the reduction reaction between $S_2O_8^{2-}$ in the electrolyte and QDs on the electrode led to ECL emission, the decreased ECL signals resulting from target AFB_1 in the samples were recorded for quantification. We evaluated electrochemical impedance spectroscopy and ECL measurements along each step in the construction of the proposed immunosensor. After systematic optimization of crucial parameters, the ECL immunosensor exhibited a good sensitivity, with a low detection limit of 0.01 ng/mL for AFB_1 in a wide concentration range of 0.05–100 ng/mL. Testing with lotus seed samples confirmed the satisfactory selectivity, stability, and reproducibility of the developed ECL immunosensor for rapid, efficient, and sensitive detection of AFB_1 at trace levels in complex matrices. This study provides a powerful and universal analytical platform for a variety of analytes that can be used in broad applications for real-time analysis, such as food and traditional Chinese medicine safety testing, environmental pollution monitoring, and disease diagnostics.

Keywords Electrochemiluminescence immunosensor · ZnCdS@ZnS quantum dots · Label-free · Nafion · Aflatoxin B_1 · Lotus seed

Introduction

Mycotoxins are the most important naturally occurring contaminants relevant to public health and trade, occurring frequently in foods, feedstuffs, and traditional Chinese medicines (TCMs) [1, 2] to cause illness or human and animal death, which has been a universal yet serious issue all over the world. AFB_1, the secondary metabolite mainly produced by *Aspergillus* fungi, is one of the most toxic mycotoxins because of its highly hepatotoxic, oncogenic, teratogenic, mutagenic, and immunotoxic properties in human and domestic animals [1, 3–6]. It has been classified as a group 1A carcinogen to humans [7], and can be found in a wide range of matrices at trace levels [8–10]. Many countries have stipulated maximum admissible levels of AFB_1 at μg/kg or ppb level [11, 12]. Therefore, reliable methods for sensitive determination of AFB_1 are in urgent demand to meet safety requirements, monitor exposure risk, and minimize regulatory and trade losses.

Apart from traditional analytical tools for mycotoxin detection [13–15], development of a simple, easy-to-operate, and cost-effective biosensing strategy for sensitive AFB_1 detection of mycotoxins is highly desirable. Recent biosensor technologies exhibit exceptional performance capabilities [16–19] like simplicity, high specificity and sensitivity, low cost, compact size, and continuous real-time analysis. Shao et al. developed a sensitive graphene oxide and detachable nanoladders–based fluorescence turn-off biosensor, showing a limit of

✉ Lidong Zhou
ldzhou@implad.ac.cn

✉ Weijun Kong
kongwj302@126.com

[1] Institute of Medicinal Plant Development, Chinese Academy of Medical Sciences and Peking Union Medical College, Beijing 100193, China

[2] Pharmacy College, Chengdu University of Traditional Chinese Medicine, Chengdu 611137, China

[3] Integrative Medical Center, Fifth Medical Center of Chinese PLA General Hospital, Beijing 100039, China

detection (LOD) of 0.1 nM for ochratoxin A (OTA) [20]. Similarly, Zhu et al. developed a two-way colorimetric biosensor based on unmodified gold nanoparticles and a switchable double-stranded DNA concatemer for OTA detection [21]. In addition to conventional colorimetric immunosensors, electrochemiluminescence (ECL) immunosensors as an alternative and promising solution has received special attention in many fields owing to its wide dynamic concentration response range and spatial control for real-time and green measurements in miniaturized formats [22, 23]. Nevertheless, no studies have reported label-free ECL immunosensors for sensitive detection of AFB_1 in complex matrices like those of TCMs. Through the measurement of electrical signals arising from a light emission process in a redox reaction of electrogenerated reactants between the electrode and electrolyte, label-free ECL immunosensors allow for the development of simple, cheap, and disposable devices with no labels, attracting considerable interest [24, 25]. Taking these advantages into account, we have developed a label-free ECL immunosensor for AFB_1 detection in lotus seeds.

Unquestionably, new luminescent materials for signal amplification platform are in continuously increasing need for ECL immunoassays. In recent decades, various promising nanomaterials with outstanding physicochemical properties or electrical conductivity have been introduced as the luminophores for signal amplification to decrease the detection limit of immunosensors [26, 27]. Among them, semiconductor quantum dots (QDs) have been the predominant candidate of interest as they exhibit excellent tunable photoluminescence, superior biocompatibility, high ECL performance, and physical/chemical stability along with size-dependent emission spectra and narrow emission peaks [28–32]. Various kinds of QDs have been developed for the fabrication of ECL immunosensors, but, pure QDs are found to produce lower ECL signals than conventional luminescent materials [33]. To resolve this problem, core/shell heterostructures could be used to improve photostability and facilitate charge separation [34]. In addition, the use of capping agents will improve the surface state of QDs and enhance ECL emission. As a preferred capping agent, wide band gap ZnS can effectively eliminate the effect of surface defects on the luminescence efficiency of QDs. Thus, core-shell ZnCdS@ZnS QDs were chosen as the signal sources to obtain strong, stable ECL intensity for detection of AFB_1.

In order to construct a stable and sensitive ECL immunosensor, self-assembled monolayers are an easy and effective way to steadily assemble the core-shell QDs on the surface of the Au electrode. As a perfluorosulfonated polymer with outstanding film-forming properties, Nafion is commonly used to assemble inorganic or biological materials to improve the mechanical stability of the modified electrode [35, 36] and has been used successfully to assemble some conventional luminescent materials [36, 37] for sensitive target detection by ECL methods. Therefore, Nafion was used to attach core-shell ZnCdS@ZnS QDs on the desired surface of the Au electrode.

Here, a simple and easy-to-construct ZnCdS@ZnS QDs–based label-free ECL immunosensor with fewer steps of fabrication and higher sensitivity than previously reported sensors was proposed for the specific determination of AFB_1 in complex TCMs through an antigen-antibody (Ag–Ab) reaction, offering a preferable alternative to heavy and large instrument–based methods. Testing in real lotus seed samples confirmed the superiority of the newly developed ECL immunosensor for rapid, highly efficient, and sensitive detection of mycotoxins at trace levels in complex matrices, providing a powerful and universal analytical platform for quantitative detection of a variety of analytes in food and TCM safety testing, environmental pollution monitoring, and disease diagnostics.

Experimental section

Materials and chemicals

N-Hydroxysuccinimide (NHS), 1-ethyl-3-(3-dimethylaminoprophl) carbodiimide hydrochloride (EDC), potassium ferricyanide ($K_3Fe(CN)_6$), sulfuric acid, and $K_2S_2O_8$ were all purchased from Shanghai Macklin Biochemical Technology Co., Ltd. (www.macklin.bioon.com, Shanghai, China). ZnCdS@ZnS QDs was obtained from Xingzi New Material Technology Development Co., Ltd. (www.xznanomat.com, Shanghai, China). 5% Nafion was purchased from Shanghai Hesen Electric Co., Ltd. (www.hesen.cn, Shanghai, China). Twenty-five micrograms per milliliter of aflatoxin B_1 (AFB_1) standard solution was supplied by Pribolab Company (www.pribolab.cn, Singapore) and kept at − 20 °C in the dark. Murine monoclonal antibodies of AFB_1 (anti-AFB_1 Abs, 1.0 mg/mL, stored in PBS solution) was acquired from Shandong Lvdu Bio—Science & Technology Co., Ltd. (www.lvdu.net, Shandong, China). A 0.1 M phosphate-buffered saline (PBS) (pH 7.4) was prepared by mixing solutions of 0.1 M Na_2HPO_4 and 0.1 M NaH_2PO_4 and then adjusting the pH with 0.1 M NaOH. The 0.01 M PBST (pH 7.4) obtained from supplementing 0.01 M PBS with 0.05% Tween-20 as the washing buffer and 0.01 M PBS was purchased from Solarbio Science & Technology Co., Ltd. (www.solarbio.com, Beijing, China). All the chemicals were of analytical grade. All solutions were prepared with ultra-pure water from a Milli-Q purification system.

Preparation of standard and sample solutions

The AFB_1 standard solution (25 μg/mL) was diluted with PBS (0.01 M, pH 7.4) to obtain different

concentrations of working solutions, which were stored in the dark at − 20 °C.

Lotus seeds were crushed and sifted through 40 meshes, and 1 g powder was carefully weighed and added to 5 mL of 80% methanol solution with vortexing for 5 min. The mixed solution was then extracted on a mixing oscillator for 30 min, followed by centrifugation at 6000 rpm for 10 min. Afterwards, the supernatant was collected and diluted with 0.01 M phosphate-buffered saline (pH 7.4) solution for analysis.

Fabrication and detection principle of the ECL immunosensor

The fabrication procedure of the ECL immunosensor is listed in Scheme 1A. First, an Au electrode with a 2-mm diameter was serially polished with 1.0, 0.3, and 0.05 μm alumina slurries to obtain a mirror-like surface, then rinsed with deionized water, methanol, and deionized water, respectively. Before modification, the bare Au electrode was scanned in 5 mmol/L $[Fe(CN)_6]^{3-/4-}$ solution

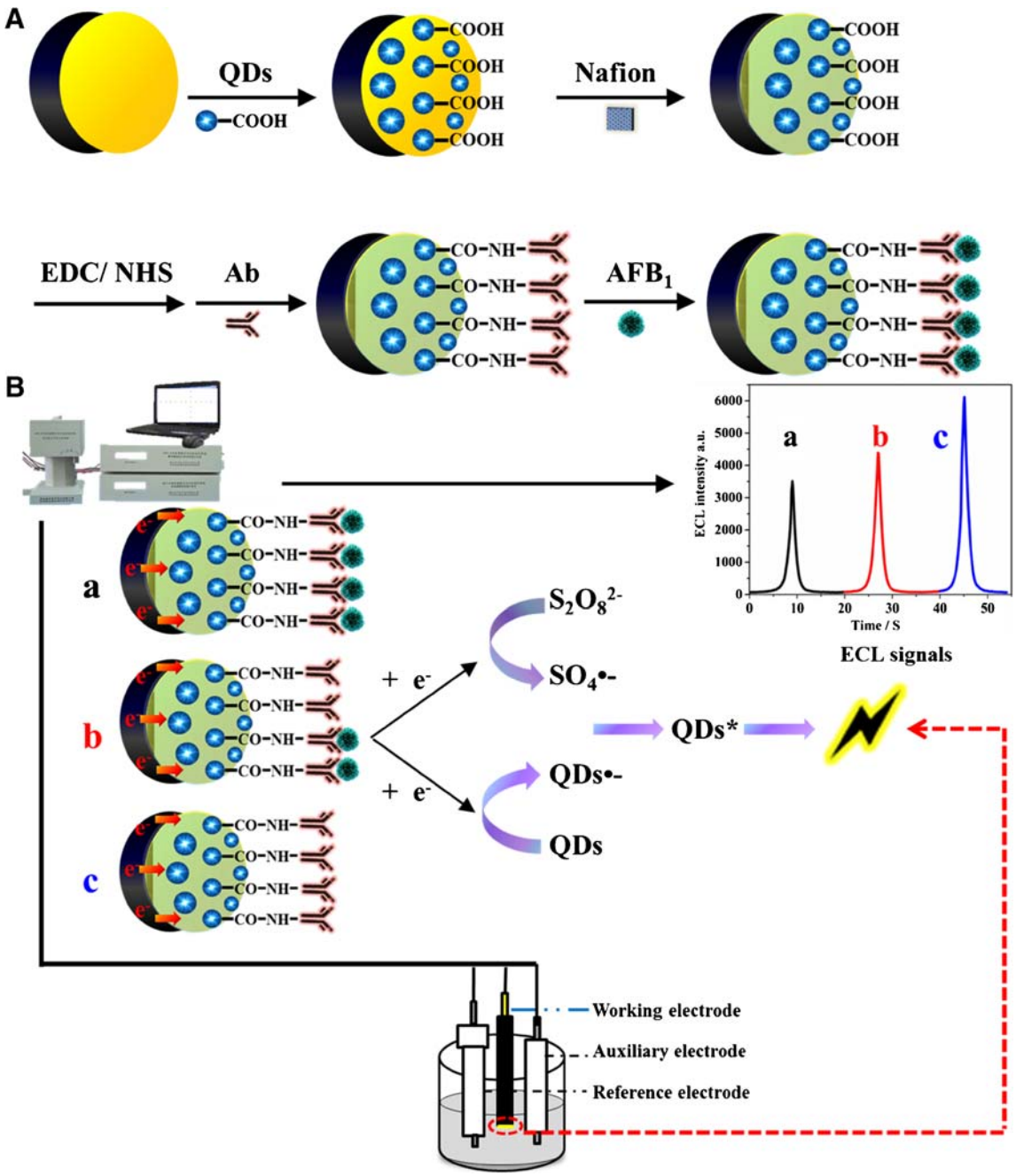

Scheme 1 (**A**) Fabrication and (**B**) detection principle of the proposed QDs-based ECL immunosensor for detection of AFB_1

containing 0.04 M KNO_3 between − 0.1 and + 0.5 V, then again in 0.5 M H_2SO_4 between + 0.3 and + 1.5 V, respectively, until reproducible signals were obtained. Then, 4 μL of ZnCdS@ZnS QDs (0.5 mg/mL) solution was dropped onto the surface of the Au electrode and allowed to dry at room temperature. Next, 3 μL of 1% Nafion solution was dropped onto the modified electrode and dried at room temperature for 30 min to form a stable film. The modified Au/QDs/Nafion electrode was then immersed in 50 μL of 0.2 M EDC + 0.1 M NHS solution as cross-linker for 20 min at 37 °C. After rinsing with PBST (pH 7.4), the electrode was incubated in 50 μL of 25 μg/mL of anti-AFB_1 antibody for 15 min at 25 °C. Finally, after rinsing with PBST (pH 7.4), the resulting electrode was used to fabricate the ECL signal probe and incubated in 50 μL of AFB_1 (Ag) standard solution with different concentrations for 30 min at 25 °C for ECL immunosensor detection. The prepared electrode was washed thoroughly with PBST (pH 7.4).

ECL detection was performed in a detector cell with 10 mL 0.1 M PBS (pH 7.4,) solution containing 0.1 M $K_2S_2O_8$ and 0.1 M KCl, and the detection principle is shown in Scheme 1B. The applied potential varied from − 0.7 to − 1.6 V at a scanning rate of 0.1 V/s and the voltage of the photomultiplier tube (PMT) was set to 800 V. $K_2S_2O_8$ was used as a co-reactant in the electrolyte. In the three-electrode system, when $S_2O_8^{2-}$ and QDs both obtained electrons from the working electrode, QDs could generate QDs* and produce ECL emission via electron transfer. The conductivity of the modified electrode decreased as AFB_1 concentration increased due to steric resistance and nonconductivity of AFB_1, thus decreasing ECL intensity.

Results and discussion

Characterization of ZnCdS@ZnS QDs

The microstructure and morphology of the ZnCdS@ZnS QDs were characterized first by transmission electron microscopy (TEM), photoluminescence (PL), and UV-Vis investigation. The TEM images in Fig. 1A illustrate that the ZnCdS@ZnS QDs exhibited smooth and uniform surfaces with good dispersibility. The average particle size of ZnCdS@ZnS QDs was approximately 8.5 nm; a promising surface area capable of hosting large amounts of antibodies to obtain ultra-sensitive ECL immunosensor probes. The PL (Fig. 1B(a)) spectrum of the ZnCdS@ZnS QDs showed a good profile along with a strong emission peak at 465 nm and the UV-Vis (Fig. 1B(b)) spectrum indicated a wide absorption band, implying their promising fluorescence properties.

Electrochemical and ECL behavior of ZnCdS@ZnS QDs

The electrochemical and ECL behaviors of ZnCdS@ZnS QDs were characterized next. The cyclic voltammogram of QDs in Fig. 2a showed that when the Au/QDs electrode was immersed in 0.1 M PBS buffer solution containing 10.1 M $K_2S_2O_8$ and 0.1 M KCl for scanning at potentials from 0 to − 1.6 V, two independent reduction peaks occurred

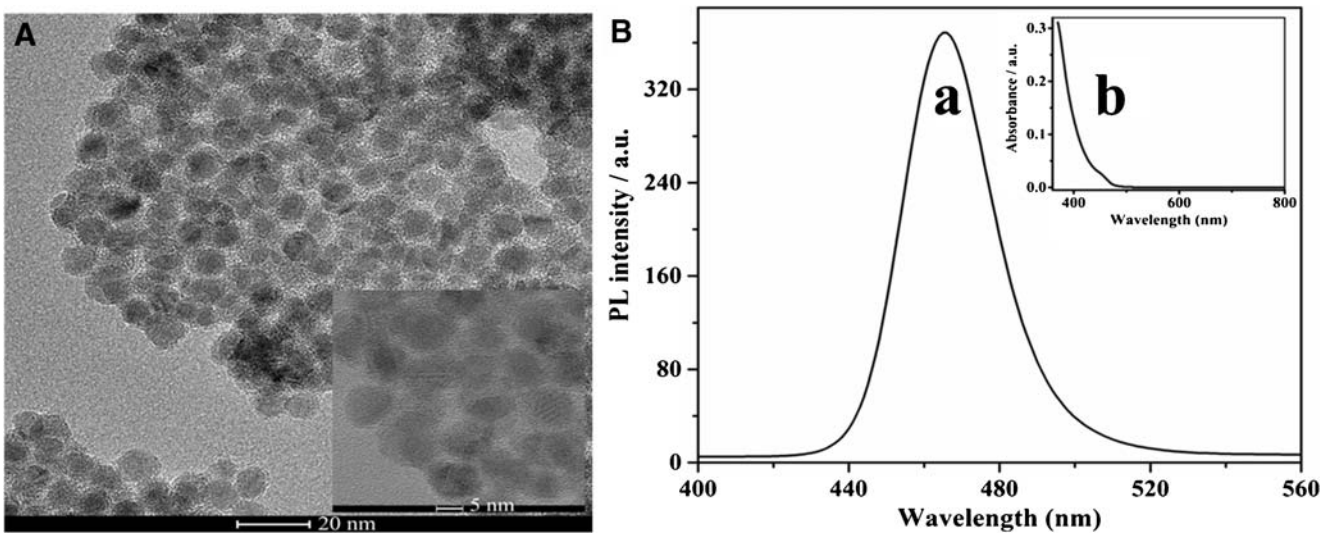

Fig. 1 (**A**) TEM image, and (**B**) PL ((*a*) PL spectrum of the ZnCdS@ZnS QDs showed a good profile along with a strong emission peak at 465 nm) and UV-Vis (inset, (*b*) UV-Vis spectrum indicated a wide absorption band, implying their promising fluorescence properties) spectra of ZnCdS@ZnS QDs

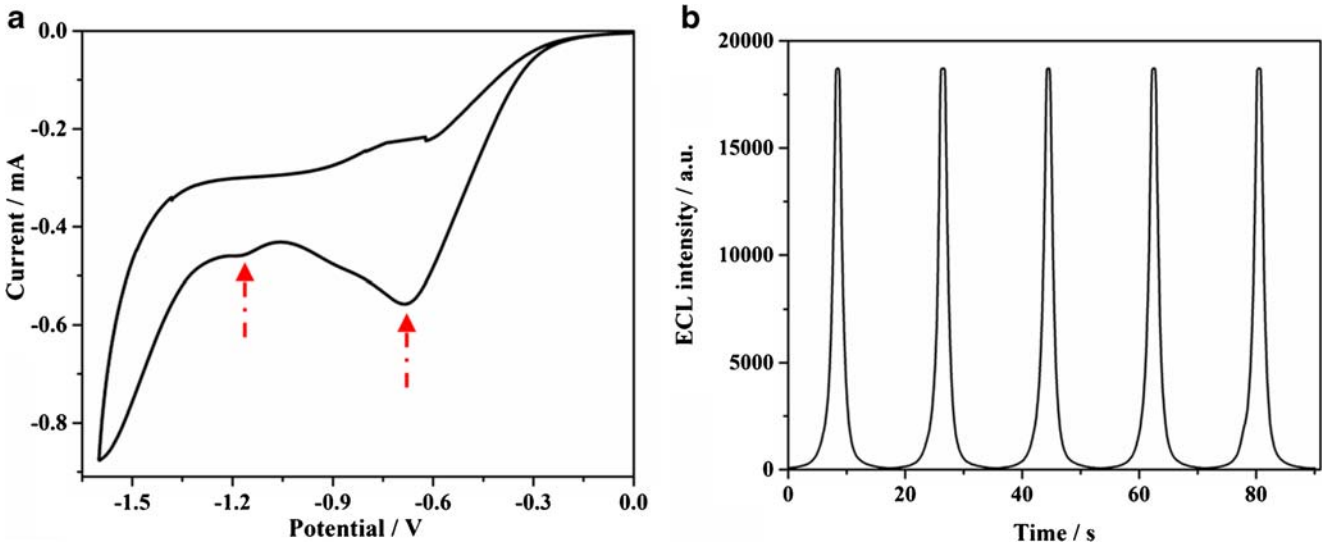

Fig. 2 (**a**) Cyclic voltammogram and (**b**) ECL signal of ZnCdS@ZnS QDs in 0.1 M PBS buffer solution containing 0.1 M $K_2S_2O_8$ and 0.1 M KCl

around − 0.68 and − 1.17 V, results of the reduction of $S_2O_8^{2-}$ and QDs, respectively. These indicate that both $S_2O_8^{2-}$ and QDs could be reduced without interference for the highly efficient generation of strong ECL signal from QDs. After continuous scanning for > 5 cycles over more than 90 s, the ZnCdS@ZnS QDs on the surface of Au electrode remained stable and capable of extremely strong ECL signal (about 18,000 a.u.) under voltage of − 0.7 to − 1.6 V in Fig. 2b, demonstrating the promising ECL performance and outstanding stability of the ZnCdS@ZnS QDs for real-world use.

In this work, during the negative potential scan, the ECL behavior of the modified Au/QDs electrode was generated by the reduction reaction between $S_2O_8^{2-}$ in the electrolyte and QDs on the electrode. The reduction of co-reactant $S_2O_8^{2-}$ produced a strong oxidant SO_4•-, while the QDs assembled on the electrode were reduced to QDs•-. Then, SO_4•- could react with electron-injected QDs•- to produce the excited state QDs* through electron transfer. Light was generated when the excited state QDs* come back to the ground-state QDs, and the ECL emission of ZnCdS@ZnS QDs was measured and listed as follows:

$$S_2O_8^{2-} + ne^- \rightarrow SO_4^{2-} + SO_4^{\bullet -}$$
$$QDs + ne^- \rightarrow nQDs^{\bullet -}$$
$$SO_4^{\bullet -} + QDs^{\bullet -} \rightarrow QDs^* + SO_4^{2-}$$
$$QDs^* \rightarrow QDs + hv$$

ECL characteristics of the developed immunosensor

To verify the feasibility of the current immunosensor, the ECL behaviors of the sensor after each modification step were characterized. As shown in Fig. 3, weak or no ECL signal (curve

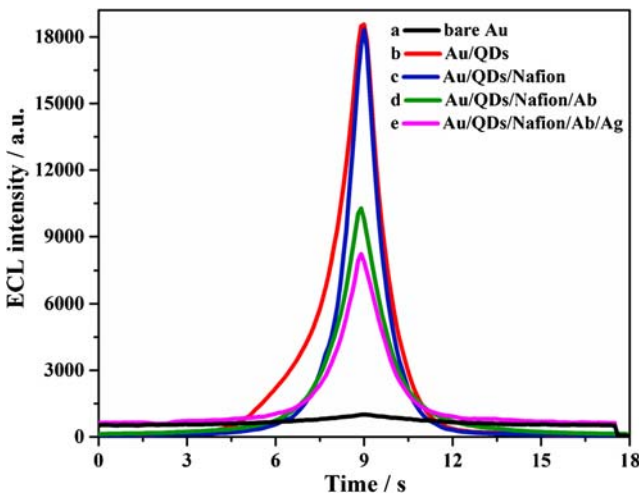

Fig. 3 ECL profile of (a) bare Au, (b) Au/QDs, (c) Au/QDs/Nafion, (d) Au/QDs/Nafion/anti-AFB_1 Ab, and (e) Au/QDs/Nafion/anti-AFB_1 Ab/Ag electrodes

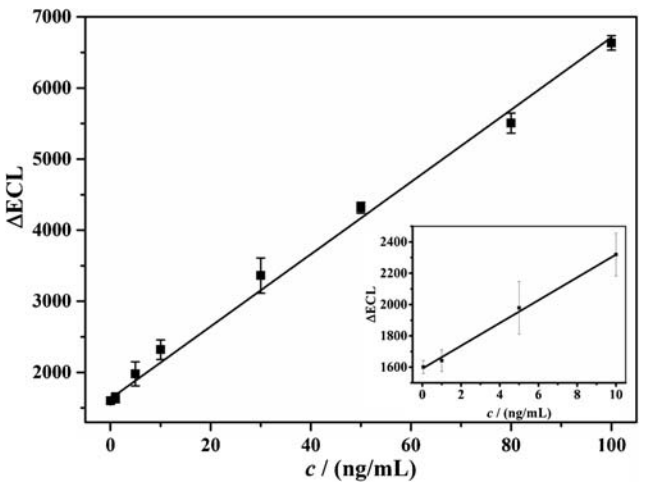

Fig. 4 Calibration ΔECL-*c* curve of the proposed ECL immunosensor. Error bars were calculated of relative standard deviation from triple parallel experiments ($n = 3$)

Table 1 Comparison of the newly-proposed ECL immunosensor with other immunosensors for the detection of AFB_1

Immunosensor	Linear range (ng/mL)	Limit of detection (ng/mL)	Matrix	Reference
Amperometric immunosensor	0.5–60	0.109	Corn	[38]
Electrochemical immunosensor	0.1–10	0.03	Olive oil	[39]
Colorimetric immunoassay	0.05–150	6.5×10^{-3}	Peanut	[40]
Photoelectrochemical immunoassay	0.01–15	2.8×10^{-3}	Peanut and corn	[41]
ZnCdS/ZnS QDs–based label-free ECL immunosensor	0.05–100	0.01	Lotus seed	This work

a) was observed from the bare Au electrode. The assembly of ZnCdS@ZnS QDs onto the surface of the bare Au electrode resulted in significant enhancement of the ECL signal (curve *b*). After modification of the Au/QDs electrode with 1% Nafion to form an Au/QDs/Nafion composite film, the ECL signal exhibited a slight change (curve *c*).

However, the conjunction of anti-AFB_1 Ab led to a noteworthy decrease in ECL intensity (curve *d*), suggesting that the anti-AFB_1 Ab could act as an electron transfer blocking layer to prevent diffusion of $S_2O_8^{2-}$ toward the electrode surface. Finally, when the Ag or target AFB_1 in tested samples was assembled on the modified Au/QDs/Nafion/anti-AFB_1 Ab electrode, the ECL signal trended toward a decrease again, and the resulting ECL signal was suitable for sensitive quantitation of AFB_1. These findings are in agreement with the EIS observations of the electrode across stepwise modification, both of which indicate that the ECL immunosensor was indeed fabricated as expected.

Analytical performance and sensitivity of the ECL immunosensor

Under the optimal experimental conditions, the ECL intensity of the described label-free ECL immunosensor response to each concentration (*c*) of AFB_1 was measured, and the corresponding ΔECL-*c* standard calibration curve following the bonding of various amounts of AFB_1 (Ag) onto the Au/QDs/Nafion/anti-AFB_1 Ab electrode is demonstrated in Fig. 4.

The ΔECL values increased linearly accordingly with increasing AFB_1 concentrations in the range of 0.05 to 100 ng/mL. The linear regression equation is $\Delta I_{ECL} = 48.817c + 1750.9$, with a correlation coefficient of 0.9975, where ΔI_{ECL} represents the difference of ECL intensity between the Au/QDs/Nafion/anti-AFB_1 Ab electrode ($c_{AFB1} = 0$) and the Au/QDs/Nafion/anti-AFB_1 Ab/Ag electrode bonded with different concentrations of AFB_1. The limit of detection (LOD) was 0.01 ng/mL ($S/N = 3$), which is much lower than other reported type immunosensors for AFB_1 detection (Table 1). In addition, compared with other reported immunosensors used in simple foods or agricultural products [38–41], the detectable range of the present ECL immunosensor is wide enough with low LOD for complex TCM matrices like lotus seeds.

The above results indicate that the newly developed ZnCdS@ZnS QDs–based label-free ECL immunosensor exhibits superior performance as a powerful tool for accurate and sensitive detection of AFB_1 in different kinds of matrices.

Selectivity, stability, and reproducibility of the ECL immunosensor

The introduction of a highly specific anti-AFB_1 Ab will improve the selectivity and specificity of any AFB_1

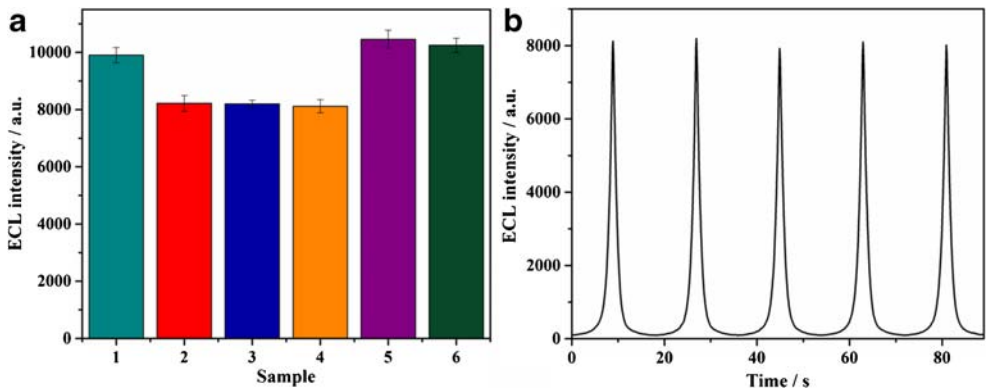

Fig. 5 (**a**) Selectivity investigation of the ECL immunosensor for AFB_1 detection against two interference mycotoxin: (1) 0 ng/mL AFB_1, (2) 0.1 ng/mL AFB_1, (3) 0.1 ng/mL AFB_1 + 10 ng/mL OTA, (4) 0.1 ng/mL AFB_1 + 10 ng/mL ZEA, (5) 10 ng/mL OTA, (6) 10 ng/mL ZEA; and (**b**) the ECL stability of the proposed ECL immunosensor under continuous cyclic voltammetry scan with 0.1 ng/mL AFB_1. Error bars were calculated of relative standard deviation from triple parallel experiments ($n = 3$)

Table 2 Recovery ($n = 5$) of the proposed ECL immunosensor for AFB_1 in real lotus seed samples

Added amount (ng/mL)	Measured amount[a] (ng/mL)	Recovery (%)	RSD (%)
5	4.960	99.20	2.15
10	10.068	100.68	2.71
20	20.194	100.97	3.78

[a] Mean value

immunoassay. To evaluate this property of the newly developed ECL immunosensor, ochratoxin A (OTA) and zearalenone (ZEA) were selected as interference mycotoxins to be tested under the same experimental conditions. As shown in Fig. 5a, the ECL signal was similar between 10 ng/mL of OTA or ZEA and the blank (without AFB_1). In contrast, the presence of 0.1 ng/mL of AFB_1 led to a similar decrease in ECL intensity compared with the addition of 10 ng/mL of OTA or ZEA, suggesting excellent selectivity and specificity of the antibody to AFB_1.

The ECL intensity of the sensor in the presence of 0.1 ng/mL of AFB_1 under continuous scans for > 5 cycles over more than 80 s was recorded (Fig. 5b). High ECL intensities (approximately 8000 a.u.) and stable signals with relative standard deviation (RSD) < 1.29% were observed, illustrating good stability of the ECL immunosensor. To evaluate the batch-to-batch variations, five batches of ECL immunosensors were fabricated in parallel for the detection of 0.1 ng/mL AFB_1 under the same optimum conditions. The RSD was < 2.88% across these batches, indicating outstanding reproducibility of the constructed ECL immunosensor.

Real sample analysis for AFB_1

The feasibility and applicability of the proposed ECL immunosensor to real-world analyses was investigated by analyzing real samples of complex matrix. Medicinal and edible lotus seed samples were spiked with three concentrations of AFB_1 (5, 10, and 20 ng/mL), followed by extraction using the preparation procedure described in the methods above. After the newly developed ECL immunosensor was incubated with lotus seed extractions, it was immersed into the electrolyte of the three-electrode system for detection of ECL signals. Decreasing ECL intensities and the ΔI_{ECL}-c regression equation were used to determine the amount of AFB_1 in the spiked lotus seed samples under the same experimental conditions. The average recovery values ($n = 5$) in Table 2 were 99.2%, 100.7%, and 101% with RSDs < 3.80%, respectively. Therefore, the proposed ECL immunosensor exhibited excellent advantages and great potential for trace detection of mycotoxins in real complex samples.

Conclusion

In this study, a simple, easy-to-fabricate, and cost-effective ZnCdS@ZnS QDs–based label-free ECL immunosensor was successfully developed and achieved selective and sensitive detection of AFB_1 in real complex samples. The superiority and advantages of this new immunosensor can be recapitulated as follows: (1) This method introduced amplification strategies based on stable assembly of QDs through the addition of Nafion solution. In addition, the ZnCdS QDs capped with ZnS is more environmentally friendly and the core-shell QDs enhanced the ECL emission to obtain strong ECL signals compared with pure QDs. (2) The use of Nafion as the film-forming solution led to the stable conjunction of an abundance of QDs, as well as anti-AFB_1 Ab and AFB_1 onto the surface of the working electrode to improve sensitivity. (3) The development of a label-free ECL immunosensor omits the need for an additional "label" step and for the use of secondary antibodies as in traditional immunoassay, which largely lowers the time and cost of analysis. (4) This method bridges sensitive ECL technology and small molecule determination at trace levels through specific antibodies for target capturing fragments and core-shell QDs for signal amplification. (5) It provides a practical platform for trace detection of multiple targets in complex TCM matrices without interference from their complicated components. In summary, the developed label-free ECL immunosensor with high sensitivity is suitable to broad applications and real-time high-throughput analysis in food and TCM safety testing, environmental pollution monitoring, and disease diagnostics.

Funding information This study is support from the National Natural Science Foundation of China (81673593 and 81973474), CAMS Innovation Fund for Medical Sciences (2016-I2M-3-010), and Beijing Natural Science Foundation (7192130).

Compliance with ethical standards

Conflict of interest The author(s) declare that they have no competing interests.

References

1. Ashiq S, Hussain M, Ahmad B (2014) Natural occurrence of mycotoxins in medicinal plants: a review. Fungal Genet Biol 66:1–10
2. Carballo D, Tolosa J, Ferrer E, Berrada H (2019) Dietary exposure assessment to mycotoxins through total diet studies: a review. Food Chem Toxicol 128:8–20
3. Matejova I, Svobodova Z, Vakula J, Mares J, Modra H (2017) Impact of mycotoxins on aquaculture fish species: a review. J World Aquacult Soc 48:186–200
4. Dai YQ, Huang KL, Zhang BY, Zhu LY, Xu WT (2017) Aflatoxin B_1-induced epigenetic alterations: An overview. Food Chem Toxicol 109:683–689
5. Zhang BY, Huang KL, Zhu LY, Luo YB, Xu WT (2017) Precision toxicology based on single cell sequencing: an evolving trend in

toxicological evaluations and mechanism exploration. Arch Toxicol 91:2539–2549
6. Yang X, Lv YJ, Huang KL, Luo YB, Xu WT (2016) Zinc inhibits aflatoxin B1-induced cytotoxicity and genotoxicity in human hepatocytes (HepG2 cells). Food Chem Toxicol 92:17–25
7. World Health Organization [WHO] and International Agency for Research on Cancer [IARC] (1993) Some naturally occurring substances: food items and constituents, heterocylic aromatic amines and mycotoxins. IARC Monogr Eval Carcinog Risks Hum 56:599
8. Anfossi L, Giovannoli C, Baggiani C (2016) Mycotoxin detection. Curr Opin Biotechnol 37:120–126
9. Cho HD, Suh JH, Feng S, Eom T, Kim J, Hyun SM, Kim J, Wang Y, Han SB (2019) Comprehensive analysis of multi-class mycotoxins in twenty different species of functional and medicinal herbs using liquid chromatography- tandem mass spectrometry. Food Control 96:517–526
10. Toman J, Ostry V, Grosse Y, Roubal T, Malir F (2018) Occurrence of ochratoxin A in *Astragalus propinquus* root and its transfer to decoction. Mycotoxin Res 34:223–227
11. European Commission (2010) Commission Regulation (EC) No 165/2010 of 26 February 2010 amending regulation (EC) no. 1881/2006 setting maximum levels for certain contaminants in foodstuffs as regards aflatoxins. Off J Eur Union 38:8–10
12. Chinese Pharmacopoeia Commission (2015) Chinese pharmacopoeia of the People's Republic of China, vol 4. Chinese Medicine Science and Technology Press, Bejing
13. Hamed AM, Moreno-González D, García-Campaña AM, Gámiz-Gracia L (2017) Determination of aflatoxins in yogurt by dispersive liquid-liquid microextraction and HPLC with photo-induced fluorescence detection. Food Anal Methods 10:516–521
14. Wei F, Liu XF, Liao XF, Shi LC, Zhang SW, Lu JH, Zhou LD, Kong WJ (2019) Simultaneous determination of 19 mycotoxins in lotus seed using a multimycotoxin UFLC-MS/MS method. J Pharm Pharmacol 71:1172–1183
15. Yang Y, Li GL, Wu D, Liu J, Li XT, Luo PJ, Hu N, Wang HL, Wu YN (2020) Recent advances on toxicity and determination methods of mycotoxins in foodstuffs. Trends Food Sci Technol 96:233–252
16. Tang DP, Lin YX, Zhou Q (2018) Carbon dots prepared from *Litchi chinensis* and modified with manganese dioxide nanosheets for use in a competitive fluorometric immunoassay for aflatoxin B_1. Microchim Acta 185:476
17. Mahmoudpour M, Dolatabadi JEN, Torbati M, Tazehkand AP, Homayouni-Rad A, de la Guardia M (2019) Nanomaterials and new biorecognition molecules based surface plasmon resonance biosensors for mycotoxin detection. Biosens Bioelectron 143:111603
18. Zhou Q, Tang DP (2020) Recent advances in photoelectrochemical biosensors for analysis of mycotoxins in food. Trends Anal Chem 124:115814
19. Sun CN, Liao XF, Huang PX, Shan GZ, Ma X, Fu LZ, Zhou LD, Kong WJ (2020) A self-assembled electrochemical immunosensor for ultra-sensitive detection of ochratoxin A in medicinal and edible malt. Food Chem 315:126289
20. Shao XL, Zhu LJ, Feng YX, Zhang YZ, Luo YB, Huang KL, Xu WT (2019) Detachable nanoladders: a new method for signal identification and their application in the detection of ochratoxin A (OTA). Anal Chim Acta 1087:113–120
21. Zhu LJ, Shao XL, Luo YB, Huang KL, Xu WT (2017) Two-way gold nanoparticle label-free sensing of specific sequence and small molecule targets using switchable concatemers. ACS Chem Biol 12:1373–1380
22. Wang HJ, Yuan YL, Zhuo Y, Chai YQ, Yuan R (2016) Sensitive electrochemiluminescence immunosensor for detection of N-acetyl-β-d-glucosaminidase based on a "light-switch" molecule combined with DNA dendrimer. Anal Chem 88:5797–5803
23. Wang YG, Zhao GH, Li XJ, Liu L, Cao W, Wei Q (2018) Electrochemiluminescent competitive immunosensor based on polyethyleneimine capped SiO_2 nanomaterials as labels to release $Ru(bpy)_3^{2+}$ fixed in 3D Cu/Ni oxalate for the detection of aflatoxin B_1. Biosens Bioelectron 101:290–296
24. Zhang HY, Miller BL (2019) Immunosensor-based label-free and multiplex detection of influenza viruses: state of the art. Biosens Bioelectron 141:111476
25. Yan Q, Cao LL, Dong H, Tan ZL, Hu YT, Liu Q, Liu H, Zhao PP, Chen L, Liu YY, Li YY, Dong YH (2019) Label-free immunosensors based on a novel multi-amplification signal strategy of TiO2-NGO/Au@Pd hetero- nanostructures. Biosens Bioelectron 127:174–180
26. Wang Q, Wang XD, Xu M, Lou XD, Xia F (2019) One-dimensional and two-dimensional nanomaterials for the detection of multiple biomolecules. Chin Chem Lett 30:1557–1564
27. Goud KY, Reddy KK, Satyanarayana M, Kummari S, Gobi VK (2020) A review on recent developments in optical and electrochemical aptamer-based assays for mycotoxins using advanced nanomaterials. Microchim Acta 187:29
28. Zhang K, Lv S, Lin ZZ, Tang DP (2017) CdS: Mn quantum dot-functionalized g-C_3N_4 nanohybrids as signal-generation tags for photoelectrochemical immunoassay of prostate specific antigen coupling DNAzyme concatamer with enzymatic biocatalytic precipitation. Biosens Bioelectron 95:34–40
29. Yang X, Yu YQ, Peng LZ, Lei YM, Chai YQ, Yuan R, Zhuo Y (2018) Strong electrochemiluminescence from MOF accelerator enriched quantum dots for enhanced sensing of trace cTnI. Anal Chem 90:3995–4002
30. Lin YX, Zhou Q, Tang DP, Niessner R, Yang HH, Knopp D (2016) Silver nanolabels-assisted ion-exchange reaction with CdTe quantum dots mediated exciton trapping for signal-on photoelectrochemical immunoassay of mycotoxins. Anal Chem 88:7858–7866
31. Li DY, Bai JK, Zhang TT, Chang C, Jin X, Huang Z, Xu B, Li QH (2019) Blue quantum dot light-emitting diodes with high luminance by improving the charge transfer balance. Chem Commun 55: 3501–3504
32. Jain S, Bharti S, Bhullar GK, Tripathi SK (2020) I-III-VI core/shell QDs: synthesis, characterizations and applications. J Lumin 219:116912
33. Ding SN, Jin Y, Chen X, Bao N (2015) Tunable electrochemiluminescence of CdSe@ZnSe quantum dots by adjusting ZnSe shell thickness. Electrochem Commun 55:30–33
34. Zeiri N, Naifar A, Abdi-Ben Nasrallah S, Said M (2019) Quadratic optical effects in ZnS/CdS/ZnS quantum dot-quantum well. Results Phys 14:102513
35. Gerhardt GA, Oke AF, Nagy G, Moghaddam B, Adams RN (1984) Nafion-coated electrodes with high selectivity for CNS electrochemistry. Brain Res 290:390–395
36. Guo JX, Lee JG, Tan T, Yeo J, Wong PW, Ghaffour N, An AK (2019) Enhanced ammonia recovery from wastewater by Nafion membrane with highly porous honeycomb nanostructure and its mechanism in membrane distillation. J Membr Sci 590:117265
37. Hosseini M, Pur MRK, Norouzi P, Moghaddam MR, Ganjali MR (2017) An enhanced electrochemiluminescence sensor modified with a $Ru(bpy)_3^{2+}/Yb_2O_3$ nanoparticle/nafion composite for the analysis of methadone samples. Mater Sci Eng C 76:483–489
38. Sharma A, Kumar A, Khan R (2018) A highly sensitive amperometric immunosensor probe based on gold nanoparticle functionalized poly(3, 4-ethylenedioxythiophene) doped with graphene oxide for efficient detection of aflatoxin B_1. Synth Met 235:136–144
39. Yu LL, Zhang Y, Hu CY, Wu H, Yang YY, Huang CS, Jia NQ (2015) Highly sensitive electrochemical impedance spectroscopy immunosensor for the detection of AFB_1 in olive oil. Food Chem 176:22–26

40. Lai WQ, Wei QH, Xu MD, Zhuang JY, Tang DP (2017) Enzyme-controlled dissolution of MnO_2 nanoflakes with enzyme cascade amplification for colorimetric immunoassay. Biosens Bioelectron 89:645–651
41. Su LS, Tong PT, Zhang LJ, Luo ZB, Fu CL, Tang DP (2019) Photoelectrochemical immunoassay of aflatoxin B_1 in foodstuff based on amorphous TiO_2 and $CsPbBr_3$ perovskite nanocrystals. Analyst 144:4880–4886